Clinical Infectious Diseases

MAJOR ARTICLE

Preferential Infection of α4β7$^+$ Memory CD4$^+$ T Cells During Early Acute Human Immunodeficiency Virus Type 1 Infection

Andrey Tokarev,[1,2] Lyle R. McKinnon,[3,4] Amélie Pagliuzza,[5] Aida Sivro,[3,4] Tosin E. Omole,[4] Eugene Kroon,[6] Nitiya Chomchey,[6] Nittaya Phanuphak,[6] Alexandra Schuetz,[1,2,7] Merlin L. Robb,[1,2] Michael A. Eller,[1,2] Jintanat Ananworanich,[1,2] Nicolas Chomont,[5] and Diane L. Bolton[1,2]; for the RV254/SEARCH010 Study Group

[1]US Military HIV Research Program, Walter Reed Army Institute of Research, Silver Spring, Maryland, USA, [2]Henry M. Jackson Foundation for the Advancement of Military Medicine, Bethesda, Maryland, USA, [3]Centre for the AIDS Programme of Research in South Africa, Durban, South Africa, [4]Department of Medical Microbiology and Infectious Diseases, University of Manitoba, Winnipeg, Canada, [5]Centre de Recherche du Centre Hospitalier de l'Université de Montréal and Department of Microbiology, Infectiology and Immunology, Université de Montréal, Montreal, Canada, [6]South East Asia Research Collaboration in HIV, Thai Red Cross AIDS Research Centre, Bangkok, Thailand, and [7]Department of Retrovirology, Armed Forces Research Institute of Medical Sciences, Bangkok, Thailand

Background. Establishment of persistent human immunodeficiency virus type 1 (HIV-1) reservoirs occurs early in infection, and biomarkers of infected CD4$^+$ T cells during acute infection are poorly defined. CD4$^+$ T cells expressing the gut homing integrin complex α4β7 are associated with HIV-1 acquisition, and are rapidly depleted from the periphery and gastrointestinal mucosa during acute HIV-1 infection.

Methods. Integrated HIV-1 DNA was quantified in peripheral blood mononuclear cells obtained from acutely (Fiebig I–III) and chronically infected individuals by sorting memory CD4$^+$ T-cell subsets lacking or expressing high levels of integrin β7 (β7^{negative} and β7^{high}, respectively). HIV-1 DNA was also assessed after 8 months of combination antiretroviral therapy (cART) initiated in Fiebig II/III individuals. Activation marker and chemokine receptor expression was determined for β7-defined subsets at acute infection and in uninfected controls.

Results. In Fiebig I, memory CD4$^+$ T cells harboring integrated HIV-1 DNA were rare in both β7^{high} and β7^{negative} subsets, with no significant difference in HIV-1 DNA copies. In Fiebig stages II/III and in chronically infected individuals, β7^{high} cells were enriched in integrated and total HIV-1 DNA compared to β7^{negative} cells. During suppressive cART, integrated HIV-1 DNA copies decreased in both β7^{negative} and β7^{high} subsets, which did not differ in DNA copies. In Fiebig II/III, integrated HIV-1 DNA in β7^{high} cells was correlated with their activation.

Conclusions. β7^{high} memory CD4$^+$ T cells are preferential targets during early HIV-1 infection, which may be due to the increased activation of these cells.

Keywords. HIV-1; acute infection; integrin β7; activation.

CD4$^+$ T cells are the main targets of human immunodeficiency virus type 1 (HIV-1) infection, and formation of early reservoirs of infected cells that persist despite years of suppressive therapy represents a major barrier to HIV-1 cure. CD4$^+$ T cells vary in susceptibility to HIV-1 infection [1], and many cellular characteristics including activation, memory status, and homing potential contribute to permissiveness [2–8]. Efforts to better define initial viral targets will improve our understanding of the establishment of HIV-1 reservoirs, with implications for both prevention and cure strategies.

We previously showed that expression of the gut homing integrin complex α4β7 on CD4$^+$ T cells was associated with HIV-1 acquisition and disease progression, and that these cells were rapidly depleted from the gastrointestinal mucosa during acute HIV-1 infection [9]. These data build on previous studies in nonhuman primates and in vitro systems suggesting increased susceptibility of α4β7$^+$ cells to HIV-1 infection [10–12], which may contribute to the rapid gut CD4$^+$ T-cell depletion observed during primary HIV-1 and simian immunodeficiency virus (SIV) infection. Preferential SIV infection of α4β7$^+$ CD4$^+$ T cells was observed within 10 days of infection in nonhuman primates, though not maintained after 2 months in untreated conditions [11]. Whether α4β7$^+$ cells are preferentially infected during acute HIV-1 infection in humans and, if so, whether this preferential infection is maintained remains unclear. To better understand

Received 24 November 2019; editorial decision 13 April 2020; accepted 24 April 2020; published online April 29, 2020.

Correspondence: D. L. Bolton, US Military HIV Research Program, 503 Grant Ave, 1N71, Silver Spring, MD 20910 (dbolton@hivresearch.org).

Clinical Infectious Diseases® 2020;71(11):e735–43

DOI: 10.1093/cid/ciaa497

the role of α4β7 in establishing HIV-1 reservoirs, we measured HIV-1 DNA levels in $\alpha4\beta7^+$ memory $CD4^+$ T cells in very early acute HIV-1 infection in the RV254 cohort in Thailand.

METHODS

Clinical Specimens

Eighteen participants from an acute HIV-1 infection cohort in Bangkok, Thailand (RV254/SEARCH010, ClinicalTrials.gov identifier NCT00796146 (Table 1) [13] were included in this study. Selected individuals were males in Fiebig stages I, II, and III (n = 6 each) [14]. Ten of the Fiebig II/III individuals with available specimens were also analyzed following 8 months of suppressive combination antiretroviral therapy (cART). One additional RV254 male participant in Fiebig stage III was analyzed by single-cell reverse-transcription quantitative polymerase chain reaction (RT-qPCR). Six chronically infected untreated age-matched Thai participants (RV304/SEARCH013, ClinicalTrials.gov identifier NCT01397669) were also included.

Cell Surface Phenotyping and Sorting

Cryopreserved peripheral blood mononuclear cells (PBMCs) were analyzed by flow cytometry (Supplementary Methods). Cryopreservation did not substantially alter β7 surface expression (Supplementary Figure 1). $CD4^+$ T cells were sorted on a BD FACS Aria II SORP (BD Biosciences) into CD45RA-defined and β7-defined populations (~10^4–10^6 cells each population) and frozen as dry cell pellets.

Quantification of Total and Integrated HIV-1 DNA

HIV-1 total and integrated DNA were quantified by nested real-time PCR (*LTR* and *alu-LTR* for total and integrated assays, respectively) as described previously [15] and in the Supplementary Methods.

Quantification of Cell-associated HIV-1 RNA

$CD4^+$ T-cell viral gene expression was measured by qPCR as previously described [16, 17], using CRF01_AE HIV-1–specific assays for spliced and unspliced RNA (Supplementary Methods). Cells were sorted by flow cytometry either at 1 cell per well or in limiting dilution to estimate RNA-positive cell frequency.

Statistical Analysis

Statistical analysis was performed using GraphPad Prism software. Analysis of unpaired and paired measurements was performed by Mann-Whitney *U* test and Wilcoxon signed-rank test, respectively. Correlations were assessed by Spearman rank correlation test. $P \leq .05$ was considered statistically significant.

RESULTS

$\beta7^{high}$ $CD4^+$ T-cell Dynamics Across HIV-1 Infection Stages

To assess the dynamics of circulating $\alpha4\beta7^+$ $CD4^+$ T cells during HIV-1 infection, we measured the expression of integrin β7 on CD45RA-negative (memory) $CD4^+$ T cells in PBMCs in viremic individuals in Fiebig I (n = 6, pre–peak viremia), Fiebig II/III (n = 12, peak or shortly after peak viremia), and chronic infection (n = 6), as well as uninfected controls (n = 6) (Table 1; Figure 1A) [14]. High surface expression of β7 on memory $CD4^+$ T cells ($\beta7^{high}$) can be a surrogate for coexpression of α4 [11, 18–20]; therefore, we interpret $\beta7^{high}$ cells as heterodimeric α4β7 receptor positive. The median frequency of $\beta7^{high}$ memory $CD4^+$ T cells was 12% (range, 7%–16%) in uninfected controls; 9% (range, 8%–17%) at Fiebig I, 9% (range, 6%–11%) at Fiebig II/III, and 10% (range, 6%–12%) in chronic infection (Figure 1B). The frequency did not differ between infection stages but was significantly lower at Fiebig II/III compared to uninfected controls ($P = .009$). Circulating $\beta7^{high}$ cells correlated inversely with plasma viremia across all infection stages ($\rho = -0.52$; $P = .01$; Figure 1C).

To assess the impact of viral suppression by cART on $\beta7^{high}$ memory $CD4^+$ T cells, $\beta7^{high}$ cells were measured longitudinally following 8 months of cART initiated at Fiebig II/III.

Table 1. Demographic and Clinical Characteristics of Uninfected Study Participants and Participants With Human Immunodeficiency Virus Type 1 Infection

Characteristic	Fiebig I	Fiebig II/III	Chronic	Uninfected
No. of participants	6	12	6	6
Days since HIV exposure,[a] median (IQR)	15 (11–17)	12 (9–24)	ND	NA
Age, y, mean (SD)	26 (5)	28 (7)	35 (10)	33 (7)
Male sex, %	100	100	100	33
HIV-1 subtype	CRF01_AE	CRF01_AE[b]	ND	NA
Viral load, copies/mL, median (IQR), × 10^3	10.5 (4–135)	490 (266–1997)	147.5 (17–594)	NA
Post-cART analysis (8 mo of cART)	ND	Yes (n = 10)	ND	NA
CD4 count, cells/μL, median (IQR)	570 (489–900)	338 (266–382)	314 (170–353)	ND
CD8 count, cells/μL, median (IQR)	505 (356–767)	519 (249–672)	1782 (592–2025)	ND

All participants were of Thai origin. HIV-1–infected participants are grouped by infection stage at the time of HIV-1 diagnosis as follows: Fiebig stage I, Fiebig stage II/III, and chronic infection.
Abbreviations: cART, combination antiretroviral therapy; HIV, human immunodeficiency virus; IQR, interquartile range; NA, not applicable; ND, not determined; SD, standard deviation.
[a]Time since HIV-1 exposure was self-reported by participants and is therefore approximate.
[b]One participant in Fiebig II/III was infected with subtype B.

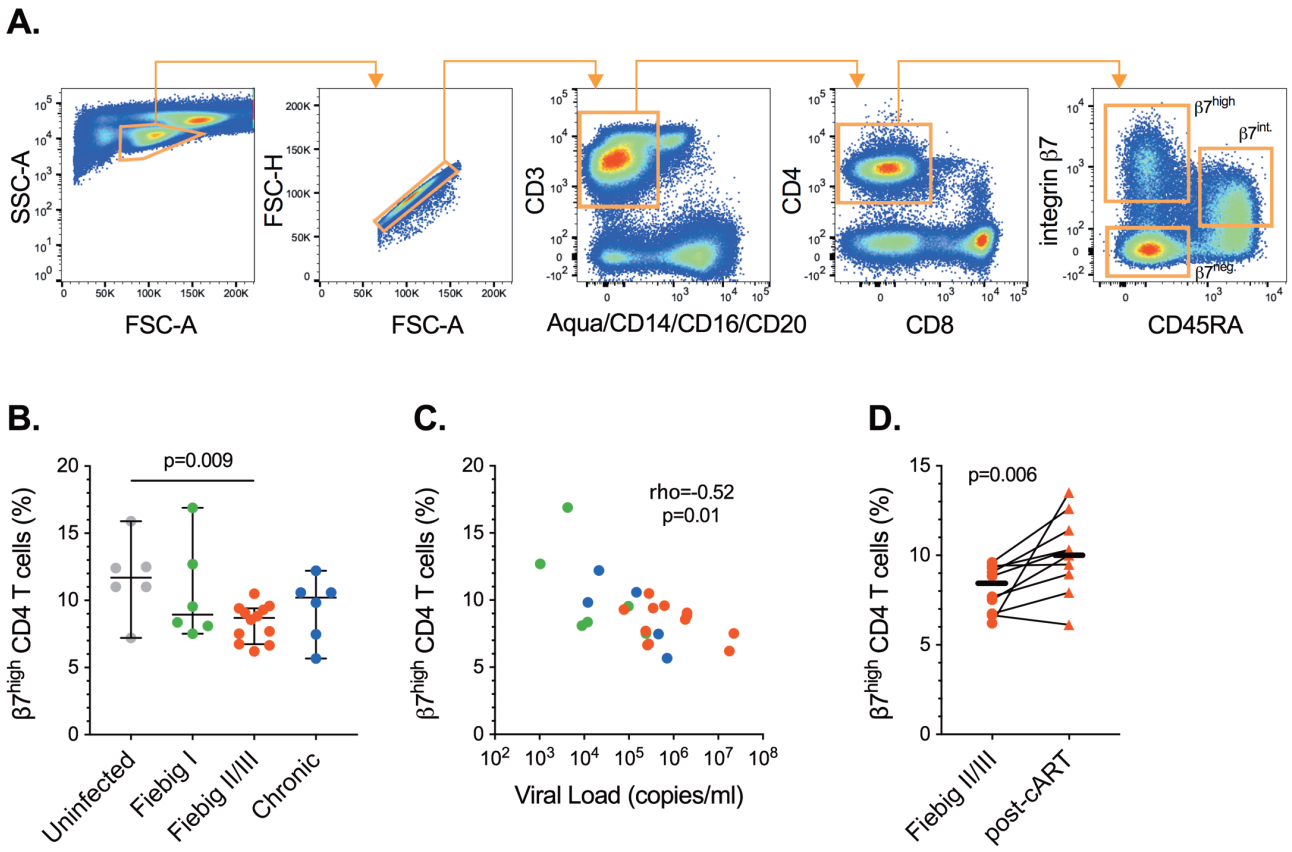

Figure 1. Frequency of $\beta7^{high}$ $CD4^+$ T cells during acute and chronic human immunodeficiency virus type 1 (HIV-1) infection. *A*, Flow cytometry gating strategy used to quantify and sort peripheral blood $CD4^+$ T-cell subsets by integrin β7 expression. Sequential gating from left to right was used to isolate the 3 populations indicated in the far right plot: $CD45RA^-$ $\beta7^{high}$, $CD45RA^-$ $\beta7^{negative}$, and $CD45RA^+\beta7^{int}$. *B*, Frequency of peripheral blood $\beta7^{high}$ $CD4^+$ T cells in uninfected, acute (Fiebig I, II/III), and chronic HIV-1–infected individuals. Median values, 95% confidence intervals, and the nonparametric Mann-Whitney test significant *P* value are shown ($P < .05$). *C*, $\beta7^{high}$ $CD4^+$ T-cell frequency is plotted vs concurrent viral load. *D*, Longitudinal analysis of $\beta7^{high}$ $CD4^+$ T-cell frequency in acute infection (Fiebig II/III) and 8 months after suppressive combination antiretroviral therapy (cART) initiation. Wilcoxon signed-rank test *P* value is shown; black bars depict median values. The colors in Figure 1C (and throughout the manuscript) reflect groups shown in Figure 1B.

Posttreatment specimens were only available for 10 of 12 individuals. Circulating $\beta7^{high}$ cell frequency increased modestly after therapy, from a median of 8% at acute infection to 10% ($P = .006$; Figure 1D). These data further support an inverse relationship between plasma viremia and $\beta7^{high}$ memory $CD4^+$ T-cell frequency.

HIV-1 DNA Enrichment in $\beta7^{high}$ Cells

To determine whether $\beta7^{high}$ cells are preferentially targeted by HIV-1 during early acute infection, we measured integrated HIV-1 DNA in sorted $\beta7^{high}$ memory $CD4^+$ T cells and their $\beta7^{negative}$ counterparts in peripheral blood (Figure 1A). During Fiebig I, integrated HIV-1 DNA burden was low in $\beta7^{high}$ cells (median, 87 copies per million [CPM] cells) and was similar between $\beta7^{high}$ and $\beta7^{negative}$ cells (Figure 2A). At Fiebig II/III, integrated HIV-1 DNA burden was considerably greater, with a median value of 760 CPM $\beta7^{high}$ cells. $\beta7^{negative}$ cells harbored less DNA; the median reduction relative to $\beta7^{high}$ cells was approximately 4-fold ($P = .003$). In chronic infection, $\beta7^{high}$ cells contained approximately 2500 integrated HIV-1 DNA CPM cells, which was approximately 2-fold greater than $\beta7^{negative}$ cells ($P = .03$). Comparing the ratio of integrated HIV-1 DNA in $\beta7^{high}$ and $\beta7^{negative}$ cells at each infection stage, the enrichment in $\beta7^{high}$ cells was greatest in Fiebig II/III (ie around peak viremia) (Figure 2B). Plasma viral load and absolute CD4 count did not correlate with this ratio.

To validate results from the integrated HIV-1 DNA assay, total HIV-1 DNA was assessed in the same cells from the Fiebig II/III donors. Additional controls included measurement in naive ($CD45RA^+$) cells expressing intermediate surface β7 ($\beta7^{int}$; Figure 1A) [9]. Similar to integrated HIV-1 DNA, total HIV-1 DNA was greatest in $\beta7^{high}$ cells (median, 6200 CPM cells; Supplementary Figure 2*A*), whereas $\beta7^{negative}$ and $\beta7^{int}$ cells contained approximately 2- and 60-fold fewer copies ($P = .03$ and $P = .0005$, respectively). Since HIV-1 infection downregulates CD4 surface expression [21], $\beta7^{high}$ and $\beta7^{negative}$ T cells double-negative for CD4 and CD8 were also analyzed (Supplementary Figure 2*B*). Median total HIV-1 DNA in $\beta7^{high}$

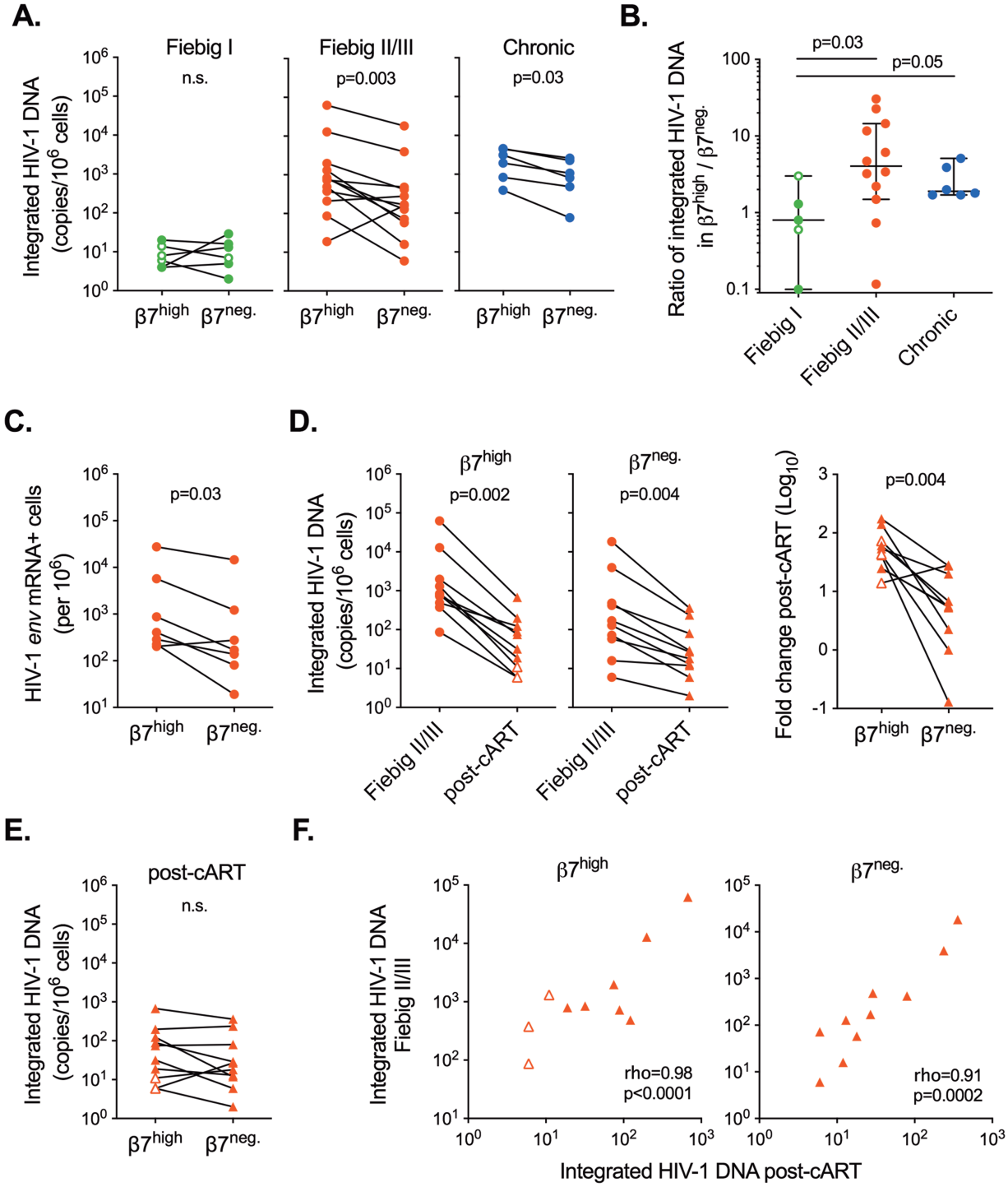

Figure 2. Human immunodeficiency virus type 1 (HIV-1) integrated DNA enrichment in integrin $\beta7^{high}$ $CD4^+$ T cells in acute and chronic infection. *A*, Peripheral blood mononuclear cell $CD4^+$ T-cell–associated integrated HIV-1 DNA in fluorescence-activated cell–sorted $\beta7^{high}$ and $\beta7^{negative}$ subsets in Fiebig I (left), Fiebig II/III (middle), and chronic (right) infection. Significant Wilcoxon test *P* values are shown ($P < .05$). *B*, Ratio of integrated HIV-1 DNA in $\beta7^{high}$ vs $\beta7^{negative}$ cells is plotted by infection stage. In 1 (Fiebig I) case, both quantitative polymerase chain reaction (qPCR) replicate values were below the limit of detection and the individual was excluded from analysis. Median values, 95% confidence intervals, and significant nonparametric Mann-Whitney test *P* values are shown. *C*, Spliced (*env*) viral RNA-positive cell frequency was estimated by limiting dilution cell sorting and reverse-transcription qPCR for $\beta7^{high}$ and $\beta7^{negative}$ $CD4^+$ T cells from Fiebig II/III-infected individuals (n = 7) for whom values were within the range of assay detection. *D*, Longitudinal integrated HIV-1 DNA in β7-defined $CD4^+$ T-cell subsets before and after 8 months of suppressive combination antiretroviral therapy (cART). Fiebig II/III and post-cART values are shown for $\beta7^{high}$ (left) and $\beta7^{negative}$ (middle) $CD4^+$ T cells; fold-change before and after cART within $\beta7^{high}$ and $\beta7^{negative}$ $CD4^+$ T cells is shown at right. *E*, $\beta7^{high}$ and $\beta7^{negative}$ $CD4^+$ T-cell–associated HIV-1 DNA values in cART-suppressed individuals. *F*, Correlation between $CD4^+$ T-cell–associated integrated HIV-1 DNA values during Fiebig II/III acute infection and 8 months post-cART in $\beta7^{high}$ (left) and $\beta7^{negative}$ (right) subsets. Negative qPCR measurements were assigned the cellular input limit of detection (LOD) value and are represented by open symbols (*A*, *D*, and *E*); calculations using an LOD value combined with a positive signal are also represented by open symbols (*B* and *F*).

double-negative T cells was approximately 40-fold less than that of the $\beta7^{high}$ $CD4^+$ T cells (160 CPM cells), and was similar between the $\beta7^{high}$ and $\beta7^{negative}$ subsets (Supplementary Figure 2C). Thus, both total and integrated HIV-1 DNA are enriched in $\beta7^{high}$ vs $\beta7^{negative}$ memory $CD4^+$ T cells, while infection is less frequent in T cells lacking surface CD4.

To determine whether viral transcription is also more common among $\beta7^{high}$ cells, we determined the frequency of cells expressing spliced viral RNA by qPCR for HIV-1 *env* in 7 of the Fiebig II/III donors [16]. The proportion of HIV-1 transcriptionally active $\beta7^{high}$ cells was approximately 400 per million cells and was 5-fold greater than that of $\beta7^{negative}$ $CD4^+$ T cells ($P = .03$; Figure 2C). Therefore, $\beta7^{high}$ cells more commonly transcribe HIV-1 during acute infection.

To assess the maintenance of $\beta7^{high}$ cell preferential infection following viral suppression, we measured integrated HIV-1 DNA longitudinally in individuals who initiated cART during acute infection Fiebig stage II/III and remained on treatment for 8 months (n = 10). As expected [22], integrated HIV-1 DNA declined after treatment in both $\beta7^{high}$ and $\beta7^{negative}$ cells (Figure 2D). The median decrease was 49-fold in $\beta7^{high}$ cells ($P = .002$) and 6-fold in $\beta7^{negative}$ cells ($P = .002$). The decline in integrated DNA was significantly greater in $\beta7^{high}$ cells ($P = .004$), indicating potentially greater decay of infected $\beta7^{high}$ than $\beta7^{negative}$ cells during therapy. Integrated HIV-1 DNA burden was approximately 20 CPM $\beta7^{high}$ cells and did not differ between $\beta7^{high}$ and $\beta7^{negative}$ cells following treatment (Figure 2E). There was a strong correlation between integrated HIV-1 DNA before and after treatment, in both $\beta7^{high}$ and $\beta7^{negative}$ subsets, consistent with previous analyses of total $CD4^+$ T cells [23] (Figure 2F).

Phenotypic Profile of $\beta7^{high}$ Memory $CD4^+$ T Cells

To understand characteristics of $\beta7^{high}$ cells that may relate to their susceptibility to HIV-1 infection, we measured surface expression of T-cell activation markers (CD38, CD69, HLA-DR, PD-1, ICOS, OX40), memory markers (CCR7, CD27), and chemokine receptors (CCR5, CXCR5, CXCR3, CCR6) implicated in HIV-1/SIV infection, in 6 uninfected controls and the Fiebig II/III acutely infected participants (n = 12; Supplementary Figure 3) [6, 11, 18, 24–31].

In uninfected individuals, differences in the expression of activation markers between $\beta7^{high}$ and $\beta7^{negative}$ cells were relatively small and varied in direction. CD38 expression was higher among $\beta7^{high}$, while HLA-DR, ICOS, and OX40 were more common on $\beta7^{negative}$ cells (all $P = .03$; Figure 3A). Surface expression of PD-1 and CD69 did not differ between $\beta7^{high}$ and $\beta7^{negative}$ cells. As expected, $CD4^+$ T-cell activation increased in acute infection relative to uninfected controls (Figure 3A), regardless of β7 profile. Comparing the β7-defined subsets during acute infection, CD38, CD69, and ICOS expression were greater among $\beta7^{high}$ than $\beta7^{negative}$ $CD4^+$ T cells, while OX40 was higher for $\beta7^{negative}$. PD-1 and HLA-DR did not differ between the subsets. Chemokine receptor expression also differed between $\beta7^{high}$ and $\beta7^{negative}$ cells in acutely infected individuals, with significantly greater CXCR5 and CXCR3 expression by $\beta7^{high}$ cells (both $P < .001$; Figure 3B). Surface expression of CCR5, CCR6, and CCR7 was similar between the β7-defined subsets. Similar trends were observed in uninfected controls. $CD38^+$ $HLA\text{-}DR^+$ double-positive cells, a more definitive measure of T-cell activation, were also increased among $\beta7^{high}$ cells in uninfected controls and at Fiebig II/III ($P = .03$ and $P = .001$, respectively; Figure 3C). Thus, $\beta7^{high}$ cells tend to display a more activated phenotype than $\beta7^{negative}$ cells, particularly during acute HIV-1 infection, potentially predisposing $\beta7^{high}$ cells to HIV-1 infection.

$\beta7^{high}$ cells were also enriched for peripheral T follicular helper ($CXCR5^+PD\text{-}1^+$) and Th1/Th17 ($CXCR3^+CCR6^+$) cells relative to $\beta7^{negative}$ cells, mirroring the distribution of cells positive for the individual markers, CXCR5 and CXCR3, and was consistent between infected and uninfected individuals (Figure 3C). Memory status did not differ between $\beta7^{high}$ and $\beta7^{negative}$ subsets among uninfected controls, with comparable central ($CCR7^+CD27^+$), transitional ($CCR7^-CD27^+$), and effector ($CCR7^-CD27^-$) memory frequencies. In contrast, in acute infection, the proportion of central and transitional memory cells among $\beta7^{high}$ cells was greater than that among $\beta7^{negative}$ cells, while effector memory predominated among $\beta7^{negative}$ cells. This suggests that effector memory $\beta7^{high}$ cells are preferentially depleted during acute infection, though acquisition or maintenance of a more long-lived memory phenotype by $\beta7^{high}$ cells relative to $\beta7^{negative}$ cells is also possible.

$\beta7^{high}$ $CD4^+$ T-cell Activation and HIV-1 Burden

We explored the relationship between the extent of $\beta7^{high}$ $CD4^+$ T-cell activation and the amount of $\beta7^{high}$ $CD4^+$ T-cell–associated HIV-1 DNA in the Fiebig II/III acutely infected individuals. Integrated HIV-1 DNA in $\beta7^{high}$ cells was highly correlated with the proportion of $\beta7^{high}$ cells expressing CD38 ($P = .006$; Figure 4A). $ICOS^+$ and $PD\text{-}1^+$ $\beta7^{high}$ cells were also associated with integrated HIV-1 DNA copies ($P = .05$ and $P = .03$, respectively), while a similar trend was observed for $HLA\text{-}DR^+$ and $CD38^+HLA\text{-}DR^+$ double-positive $\beta7^{high}$ cells (both $P = .06$; Figure 4A and data not shown). Therefore, the general activation state of $\beta7^{high}$ cells is highly linked with their infection burden.

To determine whether the increased level of CD38 on $\beta7^{high}$ cells is related to HIV-1 infection at the individual cell level, single $CD4^+$ T cells were assessed for combined surface activation marker expression and viral RNA. PBMCs from 2 Fiebig III donors with a high frequency of infected cells were surface stained and sorted by flow cytometry for single-cell HIV-1 RT-qPCR (Figure 4B) [16, 17]. Cells qualitatively positive for

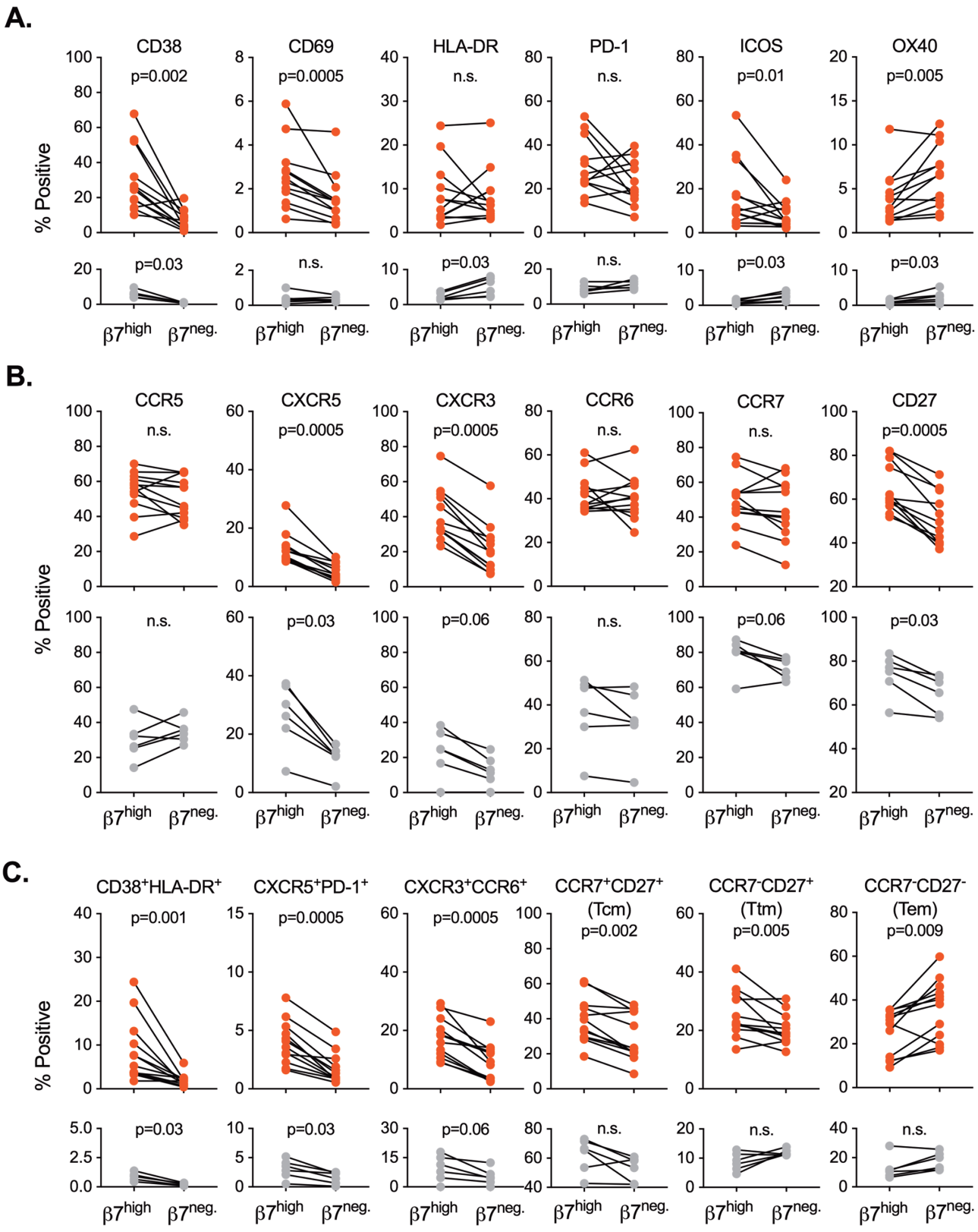

Figure 3. Activation marker and chemokine receptor expression by $\beta7^{high}$ $CD4^+$ T cells. Flow cytometric analysis of surface protein expression on $\beta7^{negative}$ and $\beta7^{high}$ $CD4^+$ T cells from peripheral blood mononuclear cells of Fiebig II/III participants with human immunodeficiency virus type 1 infection (top) and uninfected (bottom) individuals. The frequency of cells positive for the indicated activation marker (*A*) and chemokine receptor (*B*) within $\beta7^{high}$ and $\beta7^{negative}$ subsets is plotted for each participant. *C*, Frequency of cells double-positive for the indicated combination of markers is plotted as in *A* and *B*. For each graph, nonparametric Wilcoxon signed-rank test significant and trending *P* values are shown. Abbreviations: n.s., not significant; Tcm, central memory T cells; Tem, effector memory T cells; Ttm, transitional memory T cells.

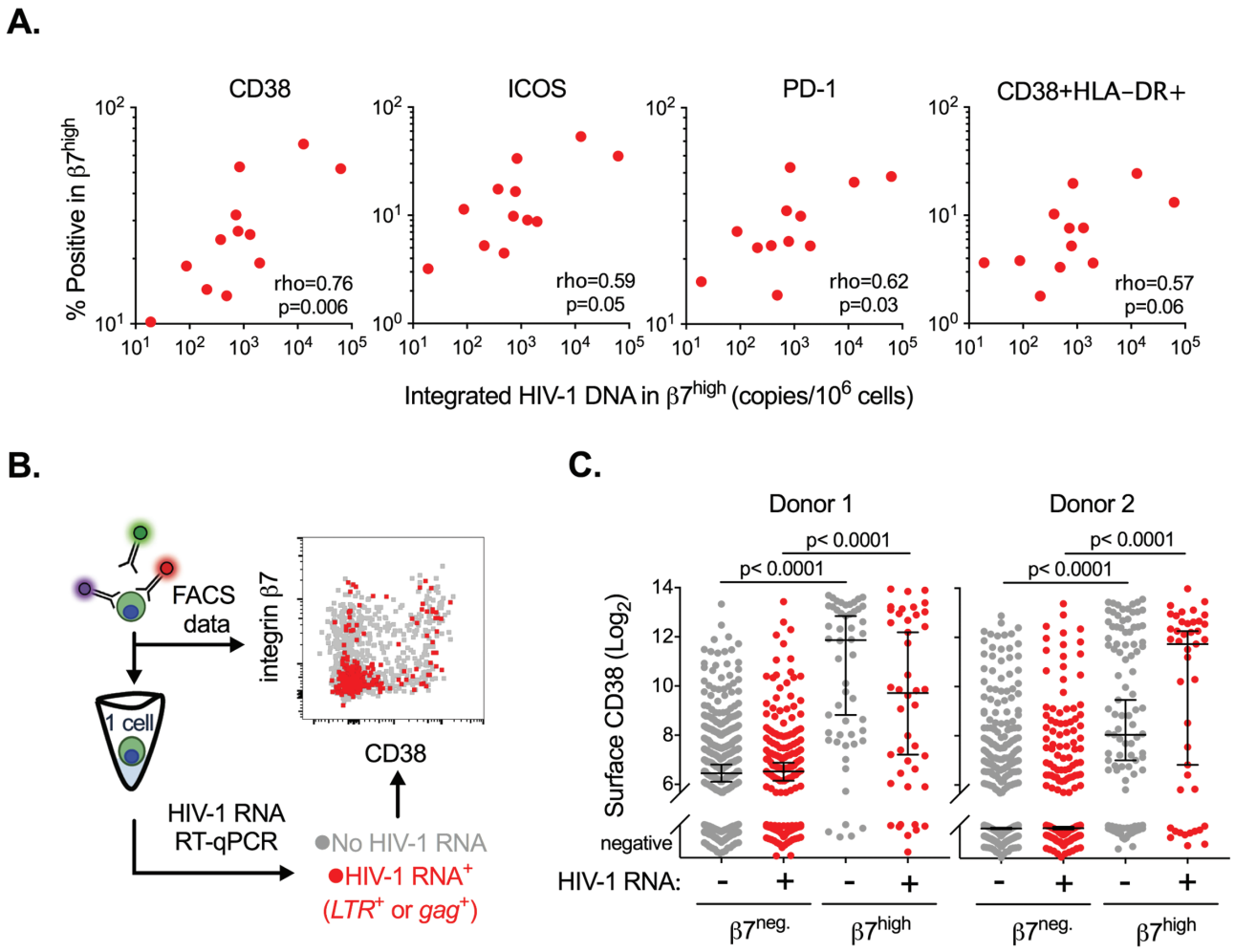

Figure 4. Relationship between $\beta7^{high}$ $CD4^+$ T-cell activation and cell-associated virus. *A*, Correlation between the frequency of $\beta7^{high}$ $CD4^+$ T cells expressing the indicated activation marker and $\beta7^{high}$ $CD4^+$ T-cell–associated integrated human immunodeficiency virus type 1 (HIV-1) DNA in peripheral blood mononuclear cells (PBMCs) of Fiebig II/III acutely infected individuals. Spearman ρ and *P* values are shown. *B*, Schematic for single-cell HIV-1 gene and host protein analysis applied to PBMCs directly ex vivo. Surface protein expression recorded by flow cytometry for single cells deposited into multiwell plates is combined with reverse-transcription quantitative polymerase chain reaction (RT-qPCR) viral gene data for each cell by well position. *C*, Surface CD38 expression (fluorescence intensity) is plotted for $\beta7^{negative}$ and $\beta7^{high}$ $CD4^+$ T cells that either lack or contain HIV-1 RNA. Graphs depict results from 2 Fiebig III participants with a high frequency of infected cells. Cells (dots) are colored by HIV-1 RNA status assessed by *gag* and *LTR* single-cell RT-qPCR. Surface CD38 values < 50 (autofluorescence of unstained cells, "negative") are randomly distributed between 1 and 50 for visualization. Significant differences determined by nonparametric Mann-Whitney rank-sum test are indicated within like HIV-1 infection states. Median values and 95% confidence intervals are shown.

viral *LTR* or *gag* RNA by a single-copy assay (Supplementary Figure 4) were (1) broadly defined as infected, including preintegration stages; (2) approximately 10-fold more common than *env*-expressing cells; and, therefore, (3) most amenable to well-powered comparisons. $\beta7^{high}$ cells expressed more CD38 than $\beta7^{negative}$ cells regardless of HIV-1 RNA positivity (Figure 4C; n > 800 cells per donor). However, CD38 expression did not significantly differ between $HIV\text{-}1^+$ and uninfected β^{7high} cells, though a trend of increased CD38 on $HIV\text{-}1^+$ $\beta7^{high}$ was observed for 1 donor ($P = .10$). Furthermore, the frequency of gag/LTR^+ infected cells was similar between $\beta7^{high}$ and $\beta7^{negative}$ subsets ($3–4 \times 10^5$ per 10^6 cells, not shown), in contrast to *env* RNA and integrated DNA. Thus, increased activation among $\beta7^{high}$ cells is independent of cellular HIV-1 infection status defined by *gag/LTR* viral RNA.

DISCUSSION

The initial stages of HIV-1 infection are dynamic and play an important role in establishing disease progression and formation of viral reservoirs. Therefore, understanding host–virus interactions in very early infection is relevant for HIV-1 prevention and treatment strategies. Given the importance of $\alpha4\beta7^+$ $CD4^+$ T cells as HIV-1 targets, including at transmission, we hypothesized that these cells are preferentially infected during early acute HIV-1 infection. Indeed, most individuals in Fiebig II/III and chronic untreated HIV-1 infection exhibited greater

infection of $\beta7^{high}$ cells compared to $\beta7^{negative}$ memory cells. Enrichment of HIV-1 DNA in $\beta7^{high}$ $CD4^+$ T cells was not observed at Fiebig I or following suppressive cART. Spliced HIV-1 RNA, a marker of active virus transcription, was also increased in $\beta7^{high}$ cells during Fiebig II/III. High expression of β7 demarcated more activated memory $CD4^+$ T cells during acute infection, and $\beta7^{high}$ cell activation levels were associated with the HIV-1 DNA burden. Collectively, HIV-1 DNA and RNA enrichment in $\beta7^{high}$ $CD4^+$ T cells indicates a viral preference to infect and replicate in these cells, during both acute and chronic infection.

Our findings reproduce those of a rhesus macaque SIV model, in which $\alpha4\beta7^+$ cells were preferentially infected and partially depleted at peak viremia [11]. They also support our previous report of $\alpha4\beta7^+$ cell frequency predicting higher rates of HIV-1 acquisition and disease progression, and the rapid depletion of $\alpha4\beta7^+$ $CD4^+$ T cells from the gastrointestinal tract of participants from the same RV254 cohort [9]. Consistent with Sivro et al, depletion of circulating $\beta7^{high}$ cells was apparent at Fiebig II/III, whereas depletion of colonic $\beta7^{high}$ cells was previously observed as early as in Fiebig I, suggesting a more rapid loss of $\beta7^{high}$ cells in the colon vs blood [9]. The preferential infection of $\alpha4\beta7^+$ $CD4^+$ T cells in chronic, untreated HIV-1 is consistent with the enrichment of HIV-1 Gag protein expression among $\alpha4\beta7^+$ $CD4^+$ T cells in chronic infection reported previously [20], but in contrast to the macaque model, where SIV DNA content in β7-defined subsets did not differ 3 months postinfection, indicating potential differences between SIV and HIV-1 infection [11].

One limitation of the current study is the cross-sectional nature of the comparison between uninfected and acutely HIV-1–infected individuals, particularly given the high variability in $\beta7^{high}$ $CD4^+$ T-cell frequency among controls. In addition, measuring integrated HIV-1 DNA likely overestimates the size of the replication competent reservoir due to the inability of this assay to discriminate between intact and defective proviruses [32, 33]. However, defective virus is likely less abundant in this early acute cohort than during chronic or late acute HIV-1 given the limited duration of viral replication and the limited number of defects that accumulated in this relatively short period of time. Moreover, due to the exceptionally small size of viral reservoirs in this early acute infection cohort, proviral DNA measurements are the most robust and sensitive approach for quantifying infection [34]. Another possible limitation is that given the slight reduction in $\beta7^{high}$ $CD4^+$ T cells in PBMCs following cryopreservation suggesting labile β7 expression, our results may underestimate HIV-1 DNA enrichment in these cells in vivo.

The mechanism behind this preferential targeting remains incompletely understood. In the present work, $\beta7^{high}$ $CD4^+$ T cells of uninfected individuals overlapped with activated and peripheral T follicular helper cells, both of which are associated with susceptibility to HIV-1 [6, 30, 35]. During acute infection, activation markers were substantially upregulated on $\beta7^{high}$ cells, and generally to a greater extent than that observed for $\beta7^{negative}$ cells, indicating heightened activation of the $\beta7^{high}$ subset. The frequency of Th1/Th17 and transitional and central memory cells, all previously shown to be preferentially infected [28, 36], are also elevated among $\beta7^{high}$ cells. Another possibility is that $\beta7^{high}$ effector memory cells were selectively infected and depleted. Notably, of all surface markers tested, only markers of activation were correlated with integrated HIV-1 DNA within $\beta7^{high}$ cells, suggesting that activation state drives $\beta7^{high}$ cell HIV-1 susceptibility in acute infection. Increased activation of $\beta7^{high}$ cells was independent of early or abortive infection of these cells determined by the presence of *LTR* or *gag* RNA. It remains to be determined if increased activation of $\beta7^{high}$ cells is associated with transcriptionally active cellular infection. In the setting of chronic HIV-1, the mechanism(s) underlying HIV-1 DNA enrichment in $\beta7^{high}$ cells may differ from that of acute infection. For example, greater persistence of $\beta7^{high}$ infected cells may also contribute. Together these data support a model whereby $\alpha4\beta7^+$ $CD4^+$ T cells are inherently more susceptible to HIV-1 compared to α4β7-negative cells and become preferentially activated and infected during the rise of HIV-1 viremia in early infection.

The low frequency of $\beta7^{high}$ $CD4^+$ T cells in blood, 5%–15% of total $CD4^+$ T cells, observed here and previously [9] indicates that despite virus enrichment in these cells compared to the other β7-defined populations, the majority of infected cells are present outside of this subset. This provides a potential explanation for lack of therapeutic efficacy of α4β7-specific antibody in the setting of treatment interruption reported recently in rhesus macaques [37–39]. However, mutations in SIV *env* observed following anti-α4β7 therapy are consistent with HIV/SIV preference for this receptor (personal communication, M. Roederer). The proportion of $\beta7^{high}$ $CD4^+$ T cells in the gut of uninfected individuals is significantly higher (~30%) than that observed in peripheral blood, and further studies are required to evaluate the efficacy of α4β7 targeting in prevention of mucosal transmission [40].

In summary, our data add to a large body of evidence that $\alpha4\beta7^+$ $CD4^+$ T cells are preferred HIV-1 targets. Infection of this gut-homing subset may have important implications for HIV-1 pathogenesis, including during treatment.

Supplementary Data

Supplementary materials are available at *Clinical Infectious Diseases* online. Consisting of data provided by the authors to benefit the reader, the posted materials are not copyedited and are the sole responsibility of the authors, so questions or comments should be addressed to the corresponding author.

Notes

Acknowledgments. The authors thank the RV254/SEARCH010 study participants and members. From the South East Asia Research Collaboration in HIV (SEARCH): Donn Colby, Carlo Sacdalan, Mark de Souza, Ponpen

Tantivitayakul, Duanghathai Suttichom, Kultida Poltavee, Jintana Intasan, Tassanee Luekasemsuk, Hathairat Savadsuk, Peeriya Prueksakaew, Somporn Tipsuk, Suwanna Puttamsawin, Khunthalee Benjapornpong, Nisakorn Ratnaratorn, Kamonkan Tangnaree, Chutharat Munkong, and Rommanus Thaimanee; from the Armed Forces Research Institute of Medical Sciences (AFRIMS): Rapee Trichavaroj, Siriwat Akapirat, Robert O'Connell, Sandhya Vasan, Yuwadee Phuang-Ngern, Suchada Sukhumvittaya, and Bessara Nuntapinit. The authors also thank Vishakha Sharma, Matthew Creegan, Hiroshi Takata, Lydie Trautmann, and Suteeraporn Pinyakorn for scientific input and technical support.

Disclaimer. The views expressed are those of the authors and should not be construed to represent the positions of the United States Army, Department of Defense, or Henry M. Jackson Foundation for the Advancement of Military Medicine. The investigators have adhered to the policies for protection of human participants as prescribed in AR-70-25.

Financial support. This work was supported by a cooperative agreement (number W81XWH-18-2-0040) between the Henry M. Jackson Foundation for the Advancement of Military Medicine and the United States Department of Defense; and by an intramural grant from the Thai Red Cross AIDS Research Center. Antiretroviral therapy for RV254/SEARCH 010 participants was supported by the Thai Government Pharmaceutical Organization, Gilead, Merck, and ViiV Healthcare.

Potential conflicts of interest. J. A. previously received honoraria from Merck, ViiV Healthcare, Roche, AbbVie, and Gilead for participation in advisory meetings. N. C. reports grants from EMD Serono and Gilead, and personal fees from Gilead, outside the submitted work. All other authors report no potential conflicts to disclose. All authors have submitted the ICMJE Form for Disclosure of Potential Conflicts of Interest. Conflicts that the editors consider relevant to the content of the manuscript have been disclosed.

References

1. McKinnon LR, Kaul R. Quality and quantity: mucosal $CD4^+$ T cells and HIV susceptibility. Curr Opin HIV AIDS **2012**; 7:195–202.
2. Zhang Z, Schuler T, Zupancic M, et al. Sexual transmission and propagation of SIV and HIV in resting and activated $CD4^+$ T cells. Science **1999**; 286:1353–7.
3. Rodriguez-Garcia M, Barr FD, Crist SG, Fahey JV, Wira CR. Phenotype and susceptibility to HIV infection of $CD4^+$ Th17 cells in the human female reproductive tract. Mucosal Immunol **2014**; 7:1375–85.
4. El Hed A, Khaitan A, Kozhaya L, et al. Susceptibility of human Th17 cells to human immunodeficiency virus and their perturbation during infection. J Infect Dis **2010**; 201:843–54.
5. McKinnon LR, Nyanga B, Kim CJ, et al. Early HIV-1 infection is associated with reduced frequencies of cervical Th17 cells. J Acquir Immune Defic Syndr **2015**; 68:6–12.
6. Perreau M, Savoye AL, De Crignis E, et al. Follicular helper T cells serve as the major CD4 T cell compartment for HIV-1 infection, replication, and production. J Exp Med **2013**; 210:143–56.
7. Geldmacher C, Ngwenyama N, Schuetz A, et al. Preferential infection and depletion of *Mycobacterium tuberculosis*–specific CD4 T cells after HIV-1 infection. J Exp Med **2010**; 207:2869–81.
8. Douek DC, Brenchley JM, Betts MR, et al. HIV preferentially infects HIV-specific $CD4^+$ T cells. Nature **2002**; 417:95–8.
9. Sivro A, Schuetz A, Sheward D, et al. Integrin alpha4beta7 expression on peripheral blood CD4(+) T cells predicts HIV acquisition and disease progression outcomes. Sci Transl Med **2018**; 10:eaam6354.
10. Kader M, Bixler S, Roederer M, Veazey R, Mattapallil JJ. CD4 T cell subsets in the mucosa are $CD28^+$Ki-67^-HLA-DR-$CD69^+$ but show differential infection based on alpha4beta7 receptor expression during acute SIV infection. J Med Primatol **2009**; 38(Suppl 1):24–31.
11. Kader M, Wang X, Piatak M, et al. Alpha4(+)beta7(hi)CD4(+) memory T cells harbor most Th-17 cells and are preferentially infected during acute SIV infection. Mucosal Immunol **2009**; 2:439–49.
12. Arthos J, Cicala C, Nawaz F, et al. The role of integrin α4β7 in HIV pathogenesis and treatment. Curr HIV/AIDS Rep **2018**; 15:127–35.
13. de Souza MS, Pinyakorn S, Akapirat S, et al; RV254/SEARCH010 Study Group. Initiation of antiretroviral therapy during acute HIV-1 infection leads to a high rate of nonreactive HIV serology. Clin Infect Dis **2016**; 63:555–61.
14. Fiebig EW, Wright DJ, Rawal BD, et al. Dynamics of HIV viremia and antibody seroconversion in plasma donors: implications for diagnosis and staging of primary HIV infection. AIDS **2003**; 17:1871–9.
15. Vandergeeten C, Fromentin R, Merlini E, et al. Cross-clade ultrasensitive PCR-based assays to measure HIV persistence in large-cohort studies. J Virol **2014**; 88:12385–96.
16. Bolton DL, McGinnis K, Finak G, Chattopadhyay P, Gottardo R, Roederer M. Combined single-cell quantitation of host and SIV genes and proteins ex vivo reveals host-pathogen interactions in individual cells. PLoS Pathog **2017**; 13:e1006445.
17. Tokarev A, Creegan M, Eller MA, Roederer M, Bolton DL. Single-cell quantitation of mRNA and surface protein expression in simian immunodeficiency virus-infected $CD4^+$ T cells isolated from rhesus macaques. J Vis Exp **2018**. doi:10.3791/57776.
18. Cicala C, Martinelli E, McNally JP, et al. The integrin alpha4beta7 forms a complex with cell-surface CD4 and defines a T-cell subset that is highly susceptible to infection by HIV-1. Proc Natl Acad Sci U S A **2009**; 106:20877–82.
19. Wang X, Xu H, Gill AF, et al. Monitoring alpha4beta7 integrin expression on circulating $CD4^+$ T cells as a surrogate marker for tracking intestinal $CD4^+$ T-cell loss in SIV infection. Mucosal Immunol **2009**; 2:518–26.
20. Pardons M, Baxter AE, Massanella M, et al. Single-cell characterization and quantification of translation-competent viral reservoirs in treated and untreated HIV infection. PLoS Pathog **2019**; 15:e1007619.
21. Levesque K, Finzi A, Binette J, Cohen EA. Role of CD4 receptor down-regulation during HIV-1 infection. Curr HIV Res **2004**; 2:51–9.
22. Ananworanich J, Chomont N, Eller LA, et al; RV217 and RV254/SEARCH010 Study Groups. HIV DNA set point is rapidly established in acute HIV infection and dramatically reduced by early ART. EBioMedicine **2016**; 11:68–72.
23. Ananworanich J, Schuetz A, Vandergeeten C, et al; RV254/SEARCH 010 Study Group. Impact of multi-targeted antiretroviral treatment on gut T cell depletion and HIV reservoir seeding during acute HIV infection. PLoS One **2012**; 7:e33948.
24. Biancotto A, Iglehart SJ, Vanpouille C, et al. HIV-1 induced activation of CD4+ T cells creates new targets for HIV-1 infection in human lymphoid tissue ex vivo. Blood **2008**; 111:699–704.
25. Cheung KW, Wu T, Ho SF, et al. alpha4beta7(+) CD4(+) effector/effector memory T cells differentiate into productively and latently infected central memory T cells by transforming growth factor beta1 during HIV-1 infection. J Virol **2018**; 92:e01510-17.
26. Deng H, Liu R, Ellmeier W, et al. Identification of a major co-receptor for primary isolates of HIV-1. Nature **1996**; 381:661–6.
27. Dragic T, Litwin V, Allaway GP, et al. HIV-1 entry into $CD4^+$ cells is mediated by the chemokine receptor CC-CKR-5. Nature **1996**; 381:667–73.
28. Gosselin A, Monteiro P, Chomont N, et al. Peripheral blood $CCR4^+CCR6^+$ and $CXCR3^+CCR6^+$ $CD4^+$ T cells are highly permissive to HIV-1 infection. J Immunol **2010**; 184:1604–16.
29. Meditz AL, Haas MK, Folkvord JM, et al. HLA-DR^+ $CD38^+$ $CD4^+$ T lymphocytes have elevated CCR5 expression and produce the majority of R5-tropic HIV-1 RNA in vivo. J Virol **2011**; 85:10189–200.
30. Savarino A, Bottarel F, Malavasi F, Dianzani U. Role of CD38 in HIV-1 infection: an epiphenomenon of T-cell activation or an active player in virus/host interactions? AIDS **2000**; 14:1079–89.
31. Stevenson M, Stanwick TL, Dempsey MP, Lamonica CA. HIV-1 replication is controlled at the level of T cell activation and proviral integration. EMBO J **1990**; 9:1551–60.
32. Eriksson S, Graf EH, Dahl V, et al. Comparative analysis of measures of viral reservoirs in HIV-1 eradication studies. PLoS Pathog **2013**; 9:e1003174.
33. Ho YC, Shan L, Hosmane NN, et al. Replication-competent noninduced proviruses in the latent reservoir increase barrier to HIV-1 cure. Cell **2013**; 155:540–51.
34. Leyre L, Kroon E, Vandergeeten C, et al. Abundant HIV-infected cells in blood and tissues are rapidly cleared upon ART initiation during acute HIV infection. Sci Transl Med **2020**; 12:eaav3491.
35. Malavasi F, Funaro A, Alessio M, et al. CD38: a multi-lineage cell activation molecule with a split personality. Int J Clin Lab Res **1992**; 22:73–80.
36. Chomont N, El-Far M, Ancuta P, et al. HIV reservoir size and persistence are driven by T cell survival and homeostatic proliferation. Nat Med **2009**; 15:893–900.
37. Iwamoto N, Mason RD, Song K, et al. Blocking α4β7 integrin binding to SIV does not improve virologic control. Science **2019**; 365:1033–6.
38. Abbink P, Mercado NB, Nkolola JP, et al. Lack of therapeutic efficacy of an antibody to α4β7 in SIVmac251-infected rhesus macaques. Science **2019**; 365:1029–33.
39. Di Mascio M, Lifson JD, Srinivasula S, et al. Evaluation of an antibody to α4β7 in the control of SIVmac239-nef-stop infection. Science **2019**; 365:1025–9.
40. Byrareddy SN, Kallam B, Arthos J, et al. Targeting α4β7 integrin reduces mucosal transmission of simian immunodeficiency virus and protects gut-associated lymphoid tissue from infection. Nat Med **2014**; 20:1397–400.